

Finite- to zero-range relativistic mean-field interactions

T. Nikšić and D. Vretenar

Physics Department, Faculty of Science,

University of Zagreb, Croatia, and and

Physik-Department der Technischen Universität München, D-85748 Garching, Germany

G. A. Lalazissis

Department of Theoretical Physics, Aristotle University of Thessaloniki, GR-54124, Greece

P. Ring

Physik-Department der Technischen Universität München, D-85748 Garching, Germany

(Dated: April 25, 2022)

Abstract

We study the relation between the finite-range (meson-exchange) and zero-range (point-coupling) representations of effective nuclear interactions in the relativistic mean-field framework. Starting from the phenomenological interaction DD-ME2 with density-dependent meson-nucleon couplings, we construct a family of point-coupling effective interactions for different values of the strength parameter of the isoscalar-scalar derivative term. In the meson-exchange picture this corresponds to different values of the σ -meson mass. The parameters of the isoscalar-scalar and isovector-vector channels of the point-coupling interactions are adjusted to nuclear matter and ground-state properties of finite nuclei. By comparing results for infinite and semi-infinite nuclear matter, ground-state masses, charge radii, and collective excitations, we discuss constraints on the parameters of phenomenological point-coupling relativistic effective interaction.

PACS numbers: 21.30.Fe, 21.60.-n, 21.60.Jz

I. INTRODUCTION

The theoretical framework of nuclear energy density functionals presents the only microscopic approach to the nuclear many-body problem that can be applied over the whole nuclide chart, from light to superheavy nuclei, and from the valley of β stability to the particle drip lines. The most complete and accurate description of ground-state properties and collective excitations of medium-heavy and heavy nuclei is currently provided by self-consistent mean-field (SCMF) models, based on the Gogny interaction, the Skyrme energy functional, and the relativistic meson-exchange effective Lagrangian [1, 2]. Nuclear energy density functionals are not necessarily related to any realistic nucleon-nucleon interaction but rather represent global functionals of nucleon densities and currents. In the mean-field approximation the dynamics of the nuclear many-body system is represented by independent nucleons moving in self-consistent potentials, which correspond to the actual density (current) distribution in a given nucleus. With a small set of universal parameters adjusted to data, SCMF models have achieved a high level of accuracy in the description of nuclear structure.

In relativistic mean-field (RMF) theory, in particular, very successful models have been based on the finite-range meson-exchange representation, in which the nucleus is described as a system of Dirac nucleons coupled to exchange mesons through an effective Lagrangian. The isoscalar scalar σ meson, the isoscalar vector ω meson, and the isovector vector ρ meson build the minimal set of meson fields that, together with the electromagnetic field, is necessary for a description of bulk and single-particle nuclear properties. In addition, a quantitative treatment of nuclear matter and finite nuclei necessitates a medium dependence of effective mean-field interactions, which takes into account higher-order many-body effects. A medium dependence can either be introduced by including nonlinear meson self-interaction terms in the Lagrangian, or by assuming an explicit density dependence for the meson-nucleon couplings. The former approach has been adopted in the construction of several successful phenomenological RMF interactions, for instance, the very popular NL3 [3], or the more recent PK1, PK1R [4] and FSUGold [5] parametrizations of the effective Lagrangian. In the latter case, the density dependence of the meson-nucleon vertex functions can be parameterized from microscopic Dirac-Brueckner calculations of symmetric and asymmetric nuclear matter [6, 7, 8] or it can be phenomenological [9, 10, 11], with parameters adjusted to

data on finite nuclei and empirical properties of symmetric and asymmetric nuclear matter.

At the energy scale characteristic for nuclear binding and low-lying excited states, meson exchange (σ , ω , ρ , ...) is just a convenient representation of the effective nuclear interaction. The exchange of heavy mesons is associated with short-distance dynamics that cannot be resolved at low energies, and therefore in each channel (scalar-isoscalar, vector-isoscalar, scalar-isovector, and vector-isovector) meson exchange can be replaced by the corresponding local four-point (contact) interactions between nucleons. The self-consistent relativistic mean-field framework can be formulated in terms of point-coupling nucleon interactions. When applied in the description of finite nuclei, relativistic mean-field point-coupling (RMF-PC) models [12, 13, 14, 15, 16] produce results that are comparable to those obtained in the meson exchange picture. Of course, also in the case of contact interactions, medium effects can be taken into account by the inclusion of higher-order interaction terms, for instance, six-nucleon vertices $(\bar{\psi}\psi)^3$, and eight-nucleon vertices $(\bar{\psi}\psi)^4$ and $[(\bar{\psi}\gamma_\mu\psi)(\bar{\psi}\gamma^\mu\psi)]^2$, or it can be encoded in the effective couplings, i.e. in the density dependence of strength parameters of the interaction in the isoscalar and isovector channels. Although a number of point-coupling models have been developed over the years, it is only more recently that phenomenological parametrizations have been adjusted and applied in the description of finite nuclei on a level of accuracy comparable to that of standard meson-exchange effective interactions [16].

In a series of recent articles [17, 18, 19], concepts of effective field theory and density functional theory have been used to derive a microscopic relativistic point-coupling model of nuclear many-body dynamics constrained by in-medium QCD sum rules and chiral symmetry. The density dependence of the effective nucleon-nucleon couplings is determined from the long- and intermediate-range interactions generated by one- and two-pion exchange processes. They are computed using in-medium chiral perturbation theory, explicitly including $\Delta(1232)$ degrees of freedom [20]. Regularization dependent contributions to the energy density of nuclear matter, calculated at three-loop level, are absorbed in contact interactions with constants representing unresolved short-distance dynamics.

In this work we consider the general problem of relating the finite-range (meson-exchange) and zero-range (point-coupling) representations of effective nuclear interactions in the relativistic mean-field framework with density-dependent coupling constants. In infinite nuclear matter this is, of course, a trivial task because of constant nucleon scalar and vector den-

sities. The Klein-Gordon equations of the meson-exchange model with meson masses m_ϕ and density-dependent couplings $g_\phi(\rho)$, are replaced by the corresponding point-coupling interaction terms with strength parameters g_ϕ^2/m_ϕ^2 . In finite nuclei, however, the problem is not so simple. Because of the radial dependence of the densities, the expansion of the meson propagator in terms of $1/m_\phi^2$ leads to an infinite series of gradient terms. In practice this series has to be replaced by a finite number of terms with additional phenomenological parameters adjusted to low-energy data. A number of studies have shown that, both for finite-range and for point-coupling mean-field models, the empirical data set of ground-state properties of finite nuclei can determine only a relatively small set of parameters in the general expansion of the effective Lagrangian in powers of the fields and their derivatives. It is therefore not a priori clear how to select the set of point-coupling interaction terms that will describe structure properties at the same level of accuracy as the meson-exchange models. An approach based on concepts of effective field theory is only of limited use here because already at the lowest orders one finds more parameters than can be uniquely determined from data.

The theoretical framework of meson-exchange and point-coupling relativistic mean-field models is briefly reviewed in Sec. II. The relation between finite-range and zero-range effective interactions is investigated in Sec. III, starting from one of the modern and most accurate meson-exchange interactions with density-dependent vertices. Sec. IV summarizes the results and ends with an outlook for future studies.

II. THEORETICAL FRAMEWORK

A. Density-dependent meson-exchange models

In the relativistic mean-field approximation the ground-state of a nucleus is described by the product of self-consistent solutions of the single-nucleon Dirac equation:

$$[\gamma_\mu(i\partial^\mu - \Sigma^\mu - \Sigma_R^\mu) - (m + \Sigma_S)]\psi = 0, \quad (1)$$

which is obtained by the variation of an effective Lagrangian with respect to the nucleon spinor $\bar{\psi}$. In the usual σ , ω , and ρ meson-exchange representation, the nucleon self-energies

are defined the following relations:

$$\Sigma_S = g_\sigma \sigma , \quad (2)$$

$$\Sigma^\mu = g_\omega \omega^\mu + g_\rho \vec{\tau} \cdot \vec{\rho}^\mu + e \frac{(1 - \tau_3)}{2} A^\mu , \quad (3)$$

and the classical meson fields are solutions of the stationary Klein-Gordon equations:

$$[-\Delta + m_\sigma^2] \sigma(\mathbf{r}) = -g_\sigma(\rho_v) \rho_s(\mathbf{r}) , \quad (4)$$

$$[-\Delta + m_\omega^2] \omega^\mu(\mathbf{r}) = g_\omega(\rho_v) j^\mu(\mathbf{r}) , \quad (5)$$

$$[-\Delta + m_\rho^2] \vec{\rho}^\mu(\mathbf{r}) = g_\rho(\rho_v) \vec{j}^\mu(\mathbf{r}) , \quad (6)$$

$$-\Delta A^\mu(\mathbf{r}) = j_p^\mu(\mathbf{r}) , \quad (7)$$

for the σ meson, the ω meson, the ρ meson (vectors in isospin space are denoted by arrows), and the Poisson equation for the vector potential, respectively.

When the meson-nucleon couplings g_σ , g_ω , and g_ρ explicitly depend on the nucleon (vector) density $\rho_v = \sqrt{j_\mu j^\mu}$, with $j_\mu = \bar{\psi} \gamma_\mu \psi$, there is an additional contribution to the nucleon self-energy – the rearrangement term:

$$\Sigma_R^\mu = \frac{j^\mu}{\rho_v} \left(\frac{\partial g_\omega}{\partial \rho_v} \bar{\psi} \gamma^\nu \psi \omega_\nu + \frac{\partial g_\rho}{\partial \rho_v} \bar{\psi} \gamma^\nu \vec{\tau} \psi \vec{\rho}_\nu + \frac{\partial g_\sigma}{\partial \rho_v} \bar{\psi} \psi \sigma \right) . \quad (8)$$

The inclusion of the rearrangement self-energies is essential for the energy-momentum conservation and the thermodynamical consistency of the model (the equality of the pressure obtained from the thermodynamical definition and from the energy-momentum tensor) [6, 9].

The sources of the Klein-Gordon equations (4), (5), and (6) are the local isoscalar and isovector densities and currents

$$\rho_S(\mathbf{r}) = \sum_k v_k^2 \bar{\psi}_k(\mathbf{r}) \psi_k(\mathbf{r}) , \quad (9)$$

$$j^\mu(\mathbf{r}) = \sum_k v_k^2 \bar{\psi}_k(\mathbf{r}) \gamma^\mu \psi_k(\mathbf{r}) , \quad (10)$$

$$j_{TV}^\mu(\mathbf{r}) = \sum_k v_k^2 \bar{\psi}_k(\mathbf{r}) \gamma^\mu \tau_3 \psi_k(\mathbf{r}) , \quad (11)$$

calculated in the *no-sea* approximation: the summation runs over all occupied states in the Fermi sea, i.e., only occupied single-nucleon states with positive energy explicitly contribute to the nucleon self-energies. v_k^2 denotes the occupation factors of single-nucleon states, and because of charge conservation only the third component of the isovector current contributes.

There are basically two ways to determine the medium (nucleon density) dependence of the meson-nucleon vertex functions. In the fully microscopic approach the symmetric and asymmetric nuclear matter Dirac-Brueckner nucleon self-energies calculated, for instance, from a bare nucleon-nucleon meson-exchange potential, are mapped in the local density approximation on the mean-field self-energies that determine the single-nucleon Dirac equation (1) [6, 7, 8]. Although empirical bulk properties of infinite nuclear matter present a very good starting point, these pseudo-data cannot really constrain the model parameters on the level that is necessary for an accurate description of properties of spherical and deformed nuclei. Therefore, in a more phenomenological approach an ansatz for the density dependence is assumed, initially guided by the microscopic Dirac-Brueckner self-energies, but a certain number of parameters is further fine tuned to a more accurate data base of experimental masses and charge radii of finite nuclei. This strategy has been adopted for several very successful semiphenomenological density-dependent interactions like, for instance, TW-99 [9], DD-ME1 [10], DD-ME2 [11]. For these interactions the couplings of the σ meson and ω meson to the nucleon are assumed to be of the form:

$$g_i(\rho) = g_i(\rho_{sat})f_i(x) \quad \text{for } i = \sigma, \omega, \quad (12)$$

where

$$f_i(x) = a_i \frac{1 + b_i(x + d_i)^2}{1 + c_i(x + d_i)^2} \quad (13)$$

is a function of $x = \rho/\rho_{sat}$, and ρ_{sat} denotes the nucleon density at saturation in symmetric nuclear matter. The eight real parameters in Eq. (13) are not independent. Five constraints: $f_i(1) = 1$, $f''_\sigma(1) = f''_\omega(1)$, and $f''_i(0) = 0$, reduce the number of independent parameters to three. Three additional parameters in the isoscalar channel are $g_\sigma(\rho_{sat})$, $g_\omega(\rho_{sat})$, and m_σ – the mass of the phenomenological σ meson. For the ρ meson coupling the functional form of the density dependence is suggested by Dirac-Brueckner calculations of asymmetric nuclear matter [7]:

$$g_\rho(\rho) = g_\rho(\rho_{sat}) \exp[-a_\rho(x - 1)], \quad (14)$$

and the isovector channel is parameterized by $g_\rho(\rho_{sat})$ and a_ρ . Bare values are used for the masses of the ω and ρ mesons: $m_\omega = 783$ MeV and $m_\rho = 763$ MeV.

The eight independent parameters are adjusted to the properties of symmetric and asymmetric nuclear matter, binding energies, charge radii, and neutron radii of spherical nuclei.

In particular, in Ref. [11] we have introduced the density-dependent effective interaction DD-ME2, which has been tested in the calculation of ground-state properties of large set of spherical and deformed nuclei. An excellent agreement with data has been obtained for binding energies, charge isotope shifts, and quadrupole deformations. When used in the relativistic RPA, DD-ME2 reproduces with high accuracy data on isoscalar and isovector collective excitations [11, 21].

B. An equivalent point-coupling model

The basic building blocks of a relativistic point-coupling (PC) Lagrangian are the densities and currents bilinear in the Dirac spinor field ψ of the nucleon:

$$\bar{\psi}\mathcal{O}_\tau\Gamma\psi, \quad \mathcal{O}_\tau \in \{1, \tau_i\}, \quad \Gamma \in \{1, \gamma_\mu, \gamma_5, \gamma_5\gamma_m u, \sigma_{\mu\nu}\}. \quad (15)$$

Here τ_i are the isospin Pauli matrices and Γ generically denotes the Dirac matrices. The interaction terms of the Lagrangian are products of these bilinears. In principle, a general effective Lagrangian can be written as a power series in the currents $\bar{\psi}\mathcal{O}_\tau\Gamma\psi$ and their derivatives. The well-known problem, however, is that properties of symmetric and asymmetric nuclear matter, as well ground-state data of finite nuclei, can constrain only a small subset of interaction terms, and the choice of this set is not unique. To build an RMF density-dependent point coupling model that will be equivalent to the standard meson-exchange picture, we start with the following Lagrangian:

$$\begin{aligned} \mathcal{L} = & \bar{\psi}(i\gamma \cdot \partial - m)\psi \\ & - \frac{1}{2}\alpha_S(\hat{\rho})(\bar{\psi}\psi)(\bar{\psi}\psi) - \frac{1}{2}\alpha_V(\hat{\rho})(\bar{\psi}\gamma^\mu\psi)(\bar{\psi}\gamma_\mu\psi) - \frac{1}{2}\alpha_{TV}(\hat{\rho})(\bar{\psi}\vec{\tau}\gamma^\mu\psi)(\bar{\psi}\vec{\tau}\gamma_\mu\psi) \\ & - \frac{1}{2}\delta_S(\partial_\nu\bar{\psi}\psi)(\partial^\nu\bar{\psi}\psi) - e\bar{\psi}\gamma \cdot A\frac{(1-\tau_3)}{2}\psi. \end{aligned} \quad (16)$$

In addition to the free-nucleon Lagrangian and the four-fermion interaction terms in the isoscalar-scalar, the isoscalar-vector and the isovector-vector channels, when applied to finite nuclei the model must include the coupling of the protons to the electromagnetic field, and derivative terms. The latter account for leading effects of finite-range interactions that are important for a quantitative description of nuclear density distributions, e.g. nuclear radii. One can, of course, include derivative terms in each spin-isospin channel, and even construct higher-order terms, but in practice data on charge radii constrain only a single

term, for instance $\delta_S(\partial_\nu\bar{\psi}\psi)(\partial^\nu\bar{\psi}\psi)$. Moreover, although we assume that medium many-body effects are encoded in the density dependence of the four-nucleon vertex functions, a single constant parametrizes the derivative term. This coupling has been microscopically estimated, for instance, from in-medium chiral perturbation calculation of inhomogeneous nuclear matter [20]. It has been shown that in the relevant region of nucleon densities $0.1 \text{ fm}^{-3} \leq \rho \leq 0.2 \text{ fm}^{-3}$, the coupling of the derivative term displays only a weak density dependence and can be approximated by a constant value $\delta_S \approx -0.7 \text{ fm}^4$.

From the variation of the Lagrangian Eq. (16) with respect to $\bar{\psi}$ the single-nucleon Dirac equation (1) is obtained, with the nucleon self-energies:

$$\Sigma^\mu = \alpha_V(\rho_v)j^\mu \quad (17)$$

$$\Sigma_{TV}^\mu = \alpha_{TV}(\rho_v)j_{TV}^\mu \quad (18)$$

$$\Sigma_S = \alpha_S(\rho_v)\rho_s + \delta_S\Delta\rho_s \quad (19)$$

$$\Sigma_R^\mu = \frac{1}{2} \frac{j^\mu}{\rho_v} \left\{ \frac{\partial\alpha_S}{\partial\rho}\rho_s^2 + \frac{\partial\alpha_V}{\partial\rho}j_\mu j^\mu + \frac{\partial\alpha_{TV}}{\partial\rho}j_{\mu TV}j_{TV}^\mu \right\}. \quad (20)$$

For systems with time-reversal symmetry in the ground state, i.e. even-even nuclei, the space components of all currents vanish ($\mathbf{j} = 0$), and because of charge conservation only the third component of the isospin current ($\tau_3 = -1$ for neutrons and $\tau_3 = +1$ for protons) contributes.

For the density dependence of the vertex functions we will assume the same functional forms as in the meson-exchange representation, i.e.

$$\alpha_i(\rho) = \alpha_i(\rho_{sat})f_i(x) \quad \text{for } i = S, V, \quad (21)$$

where $f_i(x)$ is given by Eq. (13), $x = \rho/\rho_{sat}$, and the exponential form for the isovector channel:

$$\alpha_{TV}(\rho) = \alpha_{TV}(\rho_{sat}) \exp[-a_{TV}(x - 1)], \quad (22)$$

with the parameters $\alpha_{TV}(\rho_{sat})$ and a_{TV} .

III. FROM MESON-EXCHANGE TO ZERO-RANGE INTERACTIONS

The link between the nucleon self-energies in the meson-exchange and point-coupling models is obtained by expanding the propagator in the Klein-Gordon equations (4-6)

$(-\Delta + m_\phi^2) \phi = \mp g_\phi \rho_\phi$ ((-) sign for the scalar field and (+) for the vector fields, respectively). If the density dependence of the coupling constant can be neglected, the self-energy originating from the field ϕ is approximately given by

$$\Sigma_\phi = \mp g_\phi \phi \approx \mp \frac{g_\phi^2}{m_\phi^2} \rho_\phi \mp \frac{g_\phi^2}{m_\phi^4} \Delta \rho_\phi + \dots \quad (23)$$

This is equivalent to the self-energy of the space-isospace channel ϕ in the point-coupling model

$$\Sigma_\phi = \alpha_\phi \rho_\phi + \delta_\phi \Delta \rho_\phi, \quad (24)$$

if we use the following mapping

$$\alpha_\phi = \mp \frac{g_\phi^2}{m_\phi^2} \quad \text{and} \quad \delta_\phi = \mp \frac{g_\phi^2}{m_\phi^4}. \quad (25)$$

We note that the mapping is exact for homogeneous nuclear matter, even for density-dependent couplings, simply because the derivative terms in Eqs. (23) and (24) vanish.

Starting from the meson-exchange density-dependent interaction DD-ME2, our goal is an equivalent point-coupling parametrization for the effective Lagrangian Eq. (16), with the density dependence of the parameters defined by Eqs. (21) and (22).

In a first step we have adjusted the parameters of the point-coupling model to reproduce the nuclear matter equation of state obtained with the DD-ME2 interaction. In Table I we collect the corresponding parameters (set A) of the point-coupling Lagrangian Eq. (16). Note that the derivative term does not contribute in the case of homogeneous nuclear matter, and therefore the parameter δ_S could not be determined. The calculated binding energy of symmetric nuclear matter, the nucleon Dirac mass, and the symmetry energy coincide with those obtained with DD-ME2 for all nucleon densities, simply because the mapping from meson-exchange to point-coupling is exact on the nuclear matter level.

To determine δ_S , we have used the parameter set A to calculate the surface thickness and surface energy of semi-infinite nuclear matter for several values of the parameter δ_S , starting from the microscopic estimate $\approx -0.7 \text{ fm}^4$. The results are summarized in Table II. Compared to the DD-ME2 values ($t = 2.108 \text{ fm}$ and $a_s = 17.72 \text{ MeV}$), the PC model predicts a larger surface thickness and considerably lower values for the surface energy. By increasing the value of $|\delta_S|$ the surface energy increases, but also larger values of the surface thickness are obtained. Note that the increase of $|\delta_S|$ corresponds to a reduction of the mass

of the fictitious σ meson in the meson exchange picture (cf. Eq. (25)), and this results in the increase of the range of the interaction. From the trend shown in Table II, obviously it is not possible to simultaneously reproduce both the surface thickness and energy of the DD-ME2 interaction. Higher-order terms in the expansion Eq. (23) simply cannot be absorbed in the renormalization of the strength of the second-order term. When applied to finite nuclei, such a PC interaction does not reproduce charge radii on the same level of agreement with data as DD-ME2, which has an rms error of only 0.017 fm when compared to data on absolute charge radii and charge isotope shifts [11]. Another possibility to increase the surface energy (note that the sign of this quantity is opposite to that of the bulk binding energy), is to reduce the nuclear matter binding energy at low densities, without changing its value at saturation density. This can be done by readjusting the parameters of the PC model. Following the same procedure that was used in Ref. [11] to adjust the interaction DD-ME2, the parameters are adjusted simultaneously to properties of nuclear matter and to binding energies, charge radii, and differences between neutron and proton radii of spherical nuclei. For nuclear matter the following “empirical” input is used: $E/A=-16$ MeV (5%), $\rho_{sat}=0.153$ fm $^{-3}$ (10%), $K_0=250$ MeV (5%), and $a_4=33$ MeV (5%). The values in parentheses correspond to the error bars used in the fitting procedure. The binding energies of finite nuclei and the charge radii (cf. Table V) are taken with an accuracy of 0.1% and 0.2%, respectively. Because of larger experimental uncertainties, the error bar used for the neutron skin is 5%. For the open-shell nuclei pairing correlations are treated in the BCS approximation with empirical pairing gaps (5-point formula).

Because the starting parameters are those of set A (cf. Table I), which is equivalent to DD-ME2 in nuclear matter, and the derivative term is included only in the isoscalar-scalar channel, our choice is to keep fixed the parameters of the isoscalar-vector channel, and to readjust only the three isoscalar-scalar (b_s , c_s , d_s), and two isovector ($\alpha_{TV}(\rho_{sat})$, a_{TV}) parameters. The fit has been performed for four fixed values of the coupling of the derivative term ranging from $\delta_s = -0.80$ fm 4 to $\delta_s = -0.86$ fm 4 , and the corresponding parameters are displayed in Table III (sets B, C, D, and E, respectively).

For all four parameter sets the resulting values for the surface thickness and surface energy of semi-infinite nuclear matter (Table IV) are much closer to those of DD-ME2. The corresponding binding energy curves of symmetric nuclear matter are plotted in Fig. 1, in comparison with the DD-ME2 equation of state (EOS). At nucleon densities $\rho \geq \rho_{sat}$ there

is virtually no difference between the five EOS, but nuclear matter is obviously less bound at low densities for the point-coupling effective interactions B, C, D, and E. In the insert of Fig. 1 we show that at low densities the differences with respect to the DD-ME2 EOS are reduced with the increase of the absolute strength of the derivative term. This is because the initial value of the surface energy (calculated with the parameter set A plus the derivative term) increases with $|\delta_S|$ (cf. Table II) and, therefore, there is less need to compensate the larger values of $|\delta_S|$ with the decrease of the nuclear matter binding energy at low densities. The same effect can be illustrated with the density dependence of the coupling functions of the interaction terms in the isoscalar-scalar channel. In Fig. 2 we display $\alpha_S(\rho)$ for the parameter sets B, C, D, and E, in comparison with $-g_\sigma^2(\rho)/m_\sigma^2$ of the DD-ME2 effective interaction. For the PC interactions the isoscalar-scalar coupling is weaker at low densities but, with the increase of $|\delta_S|$, it approaches the strength function of DD-ME2. The symmetry energy curves as functions of nucleon density for the PC parameter sets B, C, D, and E, and the meson-exchange DD-ME2 interaction are shown in Fig. 3. Here the differences are more pronounced at higher densities above saturation, but this is simply because the ground-state data used in the fit do not constrain the equations of state (symmetric and asymmetric) at higher densities. At $\rho \leq \rho_{sat}$ we note that the parabolic dependence on density is more pronounced for the DD-ME2 symmetry energy, and that all five curves intersect at $\rho \approx 0.12 \text{ fm}^{-3}$. The latter result is also well known in meson-exchange models for effective interactions with different values of the symmetry energy at saturation density.

With the readjustment of the parameters of the isoscalar-scalar channel (b_s , c_s , d_s) depending on the choice for δ_S , it is also necessary to fine-tune the two isovector parameters $\alpha_{TV}(\rho_{sat})$ and a_{TV} to ground-state properties of the selected set of spherical nuclei (cf. Table V). In Fig. 4 we show the deviations in percentage between the calculated and experimental charge radii (upper panel) and binding energies (lower panel) for the 12 spherical nuclei that have been used to adjust the parameters of sets B, C, D, and E in comparison with the results obtained with the meson-exchange interaction DD-ME2. Overall, the four PC interactions reproduce data on masses and radii on a level of accuracy comparable to that of DD-ME2: the deviations for charge radii are generally smaller than 0.5%, and the agreement of binding energies with data is better than 0.2%. An exception are the two lightest nuclei ^{16}O and ^{40}Ca , which are notoriously difficult to describe in a mean-field approach without including additional long-range correlations. From the results shown in Fig. 4 we note especially the

parameter set C for which the deviations are very close to those of DD-ME2.

Better results can be obtained if the constraint on the strength of the derivative term is released and δ_S is treated as a free adjustable parameter. In the meson-exchange picture this corresponds to fitting the mass of the σ meson, which has been standard practice in RMF models. We have thus refitted the parameters b_s , c_s , d_s , α_{TV} , a_{TV} and δ_S on the same set of data, and the resulting best-fit parameters are denoted as set F in Table III. We note that the values of the parameters of set F are, in fact, between those of sets C and D, i.e. the two parametrizations which produce best results in comparison with data (cf. Fig. 4). This is also true for the additional free parameter δ_S for which the optimal unconstrained value is -0.8342 , compared to -0.82 (set C) and -0.84 (set D). Compared to the parameter sets B, C, D, and E, the effective interaction – set F produces results that are in slightly better agreement with data, but an unexpected problem has appeared when we checked the corresponding relativistic (quasiparticle) random-phase approximation R(Q)RPA [27, 28] results for the excitation energies of collective excitations – giant resonances. Although for all five sets the calculated excitation energies of the isoscalar quadrupole and isovector dipole resonances in spherical nuclei are in very good agreement with data, on the level of accuracy comparable to that of DD-ME2 [11], the excitation energies of the isoscalar giant monopole resonances (ISGMR) are systematically above the experimental values. This is illustrated in Fig. 5 where we compare the mass dependence of the calculated ISGMR centroid energies (m_1/m_0) with the data from the TAMU [22, 23, 24] and Osaka [25, 26] compilations for medium-heavy and heavy spherical nuclei. Although the excitation energies calculated with DD-ME2 (nuclear matter compression modulus $K_{nm} = 251$ MeV) are in very good agreement with data, the values obtained with the parameter set F ($K_{nm} = 250$ MeV) are consistently higher over the whole mass range from ^{90}Zr to ^{208}Pb . This indicates that the surface incompressibility of the point-coupling model is higher than that of the corresponding meson-exchange model. It also means that to reproduce the data on ISGMR, a relativistic point-coupling interaction should have a nuclear matter compression modulus below 250 MeV. This difference is a very interesting result, because in the relativistic framework with meson-exchange interactions the interval of allowed values for K_{nm} is rather narrow. In particular, in a recent relativistic RPA analysis based on modern effective Lagrangians with explicit density dependence of the meson-nucleon vertex functions, we have shown that only effective interactions with $K_{nm} = 250 - 270$ MeV reproduce the experimental excitation

energies of ISGRM in medium-heavy and heavy nuclei and that $K_{nm} \approx 250$ MeV represents the lower limit for the nuclear matter compression modulus of relativistic mean-field interactions [29]. This result has also been confirmed by the continuum relativistic RPA analysis of isoscalar monopole strength in ^{90}Zr and ^{208}Pb of Ref. [30]. By using RMF effective Lagrangians with nonlinear meson self-interactions, the compression modulus of symmetric nuclear matter has been constrained to the range $K_{nm} = 248 \pm 8$ MeV.

The results shown in Fig. 5, however, point to a lower value for the nuclear matter incompressibility of our point-coupling interactions. We have thus readjusted the six parameters b_s , c_s , d_s , α_{TV} , a_{TV} and δ_S on the same set of data, but with the constraint on the nuclear matter compression modulus $K_{nm} = 230$ MeV. The parameters of this interaction, denoted set G, are listed in the last column of Table III, and the resulting R(Q)RPA results for the ISGMR centroids are shown in Fig. 5. The excitation energies are now much closer to the results obtained with DD-ME2, and the comparison with data shows that the point-coupling interaction could even be adjusted to a slightly lower value of K_{nm} . Now a compression modulus $K_{nm} \approx 230$ MeV is within the range of values deduced from nonrelativistic self-consistent Skyrme-Hartree-Fock plus RPA calculations [31, 32]. Because Skyrme forces belong to the class of point-coupling (contact) interactions, it would be tempting to attribute the well-known puzzle of different ranges of K_{nm} used by standard relativistic mean-field interactions (250 – 270 MeV [29, 30]), and nonrelativistic Skyrme interactions (220 – 235 MeV [31, 32]), to the fact that the former are of finite-range type (effective meson-exchange forces). However, we note that on one hand the highly successful non-relativistic finite-range Gogny forces also require $K_{nm} \leq 230$ MeV [33] and, on the other hand, it seems to be possible to construct Skyrme forces with $K_{nm} \approx 250$ MeV [32]. Therefore, even if the present analysis does not resolve the puzzle of different nuclear matter compression moduli that have been used by relativistic and non-relativistic mean-field models, it shows that the gap can be further narrowed, if not completely closed, by exploring a new class of point-coupling relativistic interactions.

For completeness, in Table V we list the results obtained with the parameter set G for the binding energies, charge radii, and differences between radii of neutron and proton density distributions of the set of 12 spherical nuclei, in comparison with the experimental values. The agreement between the calculated values and data is rather good and, except for ^{16}O and ^{40}Ca , on the same level of accuracy as DD-ME2 (cf. Table II of Ref. [11]). One has to

keep in mind, however, that in the present analysis all the point-coupling interactions were based on DD-ME2 and that we have only readjusted the isoscalar-scalar and isovector-vector channels, whereas the parameters of the isoscalar-vector interaction were kept fixed on the values obtained by mapping the DD-ME2 parameters in nuclear matter. An even better agreement with data could probably be obtained by an unconstrained fit of all interaction terms of a density-dependent point-coupling interaction.

IV. CONCLUSIONS

Models based on the self-consistent relativistic mean-field approximation have become a standard tool for the description of ground-state properties and collective excitations in spherical and deformed medium-heavy and heavy nuclei. Most applications have been based on the standard meson-exchange representation of the effective nuclear interaction, with the medium dependence determined either from microscopic Dirac-Brueckner calculations in nuclear matter, or in a phenomenological way by adjusting the meson-nucleon couplings to nuclear matter and ground-state properties of finite nuclei.

Effective field theory arguments suggest that, at the low-energy scale of nuclear structure, the picture of heavy-meson exchange associated with the largely unknown short-distance dynamics can be effectively replaced by local four-point (contact) interactions between nucleons. This is the basis of relativistic point-coupling models that, in principle, must provide a description of nuclear many-body dynamics at the level of accuracy of phenomenological meson-exchange mean-field effective interactions. Although the relation between the two representations is straightforward in nuclear matter, the situation is considerably more complicated in the description of finite nuclei. Already at the lowest order there are more point-coupling interaction terms in the four spin-isospin channels than can be constrained by available low-energy data. As in the meson-exchange picture one can, of course, resort to a microscopic description of the in-medium effective nucleon-nucleon interaction based, for instance, on chiral effective field theory. The resulting nucleon self-energies in nuclear matter can then be mapped in the local density approximation on the corresponding terms of a relativistic nuclear energy density functional. However, in a completely phenomenological approach, one makes an empirical choice of interaction terms and adjusts the parameters to nuclear matter and data on finite nuclei. Both approaches require the same number of

adjustable parameters that have to be fine tuned to low-energy data.

In this work we have considered the mapping of a highly successful phenomenological finite-range interaction with density-dependent meson-nucleon couplings (DD-ME2) on the zero-range (point-coupling) relativistic mean-field framework. We have constructed a set of point-coupling effective interactions for different values of the strength parameter of the isoscalar-scalar derivative term. In the meson-exchange representation this corresponds to different values of the mass of the phenomenological σ meson. The parameters of the density dependence of the isoscalar-scalar and isovector-vector interaction terms have then been fine-tuned to nuclear matter and ground-state properties of finite nuclei. In a comparison of the corresponding results for infinite and semi-infinite nuclear matter, ground-state masses, charge radii, and collective excitations, we have discussed constraints on the point-coupling relativistic effective interactions. It has been shown that to achieve a satisfactory description of surface properties of semi-infinite matter and nuclear charge radii, this class of point-coupling interactions must produce a slightly softer nuclear matter equation of state, compared to the ones that characterize meson-exchange interactions. Another interesting result is that, to reproduce the excitation energies of isoscalar giant monopole resonances, this type of point-coupling interaction requires a nuclear matter compression modulus of $K_{nm} \approx 230$ MeV, considerably lower than the values typically used for finite-range meson-exchange relativistic interactions, and within the range of values used by modern nonrelativistic Skyrme interactions.

ACKNOWLEDGMENTS

This work was supported in part by MZOS - project 1191005-1010, by the DFG research cluster “Origin and Structure of the Universe”, by the Alexander von Humboldt Stiftung, by Pythagoras II - EPEAEK II and EU project 80861.

-
- [1] M. Bender, P.-H. Heenen, and P.-G. Reinhard, *Rev. Mod. Phys.* 75, 121 (2003).
 - [2] D. Vretenar, A.V. Afanasjev, G.A. Lalazissis, and P. Ring, *Phys. Rep.* 409, 101 (2005).
 - [3] G. A. Lalazissis, J. König, and P. Ring, *Phys. Rev. C* 55, 540 (1997).
 - [4] W. Long, J. Meng, N. V. Giai, and S.-G. Zhou, *Phys. Rev. C* 69, 034319 (2004).

- [5] B. G. Todd-Rutel and J. Piekarewicz, *Phys. Rev. Lett.* **95**, 122501 (2005).
- [6] C. Fuchs, H. Lenske, and H.H. Wolter, *Phys. Rev. C* **52**, 3043 (1995).
- [7] F. de Jong and H. Lenske, *Phys. Rev. C* **57**, 3099 (1998).
- [8] F. Hofmann, C.M. Keil, and H. Lenske, *Phys. Rev. C* **64**, 034314 (2001).
- [9] S. Typel and H.H. Wolter, *Nucl. Phys. A* **656**, 331 (1999).
- [10] T. Nikšić, D. Vretenar, P. Finelli, and P. Ring, *Phys. Rev. C* **66**, 024306 (2002).
- [11] G.A. Lalazissis, T. Nikšić, D. Vretenar and P. Ring, *Phys. Rev. C* **71**, 024312 (2005).
- [12] D. G. Madland, B. A. Nikolaus, and T. Hoch, *Phys. Rev. C* **46**, 1757 (1992).
- [13] T. Hoch, D. Madland, P. Manakos, T. Mannel, B.A. Nikolaus, and D. Strottman, *Phys. Rep.* **242**, 253 (1994).
- [14] J. L. Friar, D. G. Madland, and B. W. Lynn, *Phys. Rev. C* **53**, 3085 (1996).
- [15] J. J. Rusnak and R. J. Furnstahl, *Nucl. Phys. A* **627**, 495 (1997).
- [16] T. Bürvenich, D. G. Madland, J. A. Maruhn, and P.-G. Reinhard, *Phys. Rev. C* **65**, 044308 (2002).
- [17] P. Finelli, N. Kaiser, D. Vretenar, and W. Weise, *Eur. Phys. J. A* **17**, 573 (2003).
- [18] P. Finelli, N. Kaiser, D. Vretenar, and W. Weise, *Nucl. Phys. A* **735**, 449 (2004).
- [19] P. Finelli, N. Kaiser, D. Vretenar, and W. Weise, *Nucl. Phys. A* **770**, 1 (2004).
- [20] S. Fritsch, N. Kaiser and W. Weise, *Nucl. Phys. A* **750**, 259 (2005).
- [21] N. Paar, D. Vretenar, E. Khan, and G. Colò, *Rep. Prog. Phys.* **70**, 1 (2007).
- [22] D. H. Youngblood, Y.-W. Lui, and H. L. Clark, *Phys. Rev. C* **55**, 2811 (1997).
- [23] D. H. Youngblood, H. L. Clark, and Y.-W. Lui, *Phys. Rev. Lett.* **82**, 691 (1999).
- [24] D. H. Youngblood, Y.-W. Lui, H. L. Clark, B. John, Y. Tokimoto, and X. Chen, *Phys. Rev. C* **69**, 034315 (2004).
- [25] M. Uchida et al., *Phys. Lett. B* **557**, 12 (2003).
- [26] M. Uchida et al., *Phys. Rev. C* **69**, 051301(R) (2004).
- [27] T. Nikšić, D. Vretenar, and P. Ring, *Phys. Rev. C* **66**, 064302 (2002).
- [28] N. Paar, P. Ring, T. Nikšić, and D. Vretenar, *Phys. Rev. C* **67**, 034312 (2003).
- [29] D. Vretenar, T. Nikšić, and P. Ring, *Phys. Rev. C* **68**, 024310 (2003).
- [30] J. Piekarewicz, *Phys. Rev. C* **69**, 041301(R) (2004).
- [31] G. Colò and N. Van Giai, *Nucl. Phys. A* **731**, 15 (2004).
- [32] G. Colò, N. Van Giai, J. Meyer, K. Bennaceur, and P. Bonche, *Phys. Rev. C* **70**, 024307

(2004).

[33] J.P. Blaizot, J.F. Berger, J. Dechargé, and M. Girod, Nucl. Phys. A 591, 435 (1995).

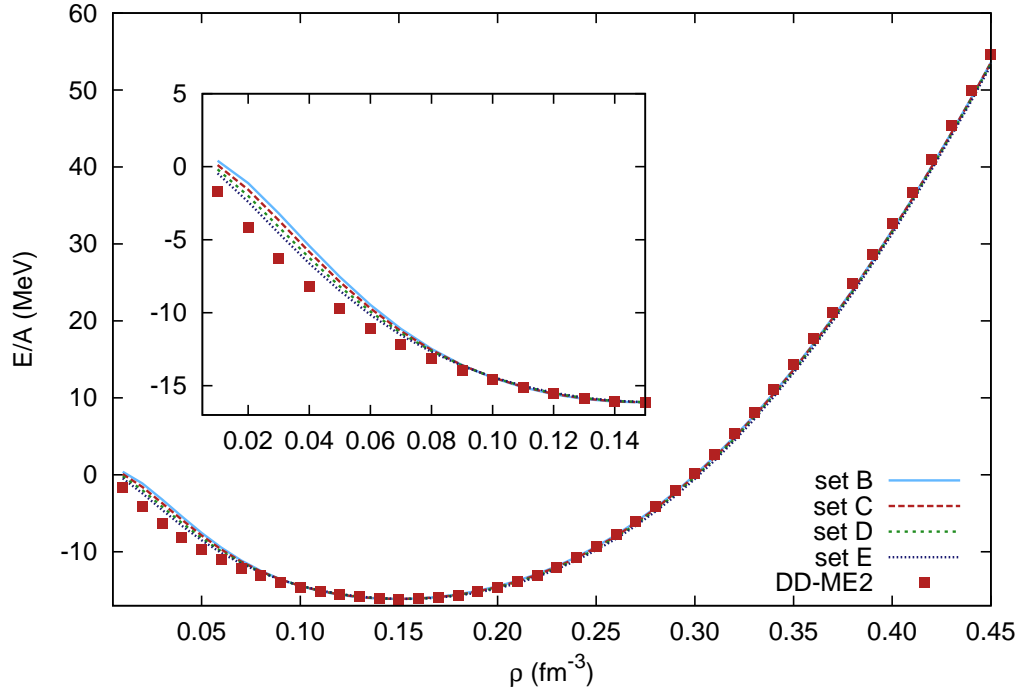


FIG. 1: The equation of state of symmetric nuclear matter (binding energy as function of nucleon density) for the meson-exchange interaction DD-ME2, and four different point-coupling effective interactions (cf. Table III). The insert highlights the EOS in the low-density region.

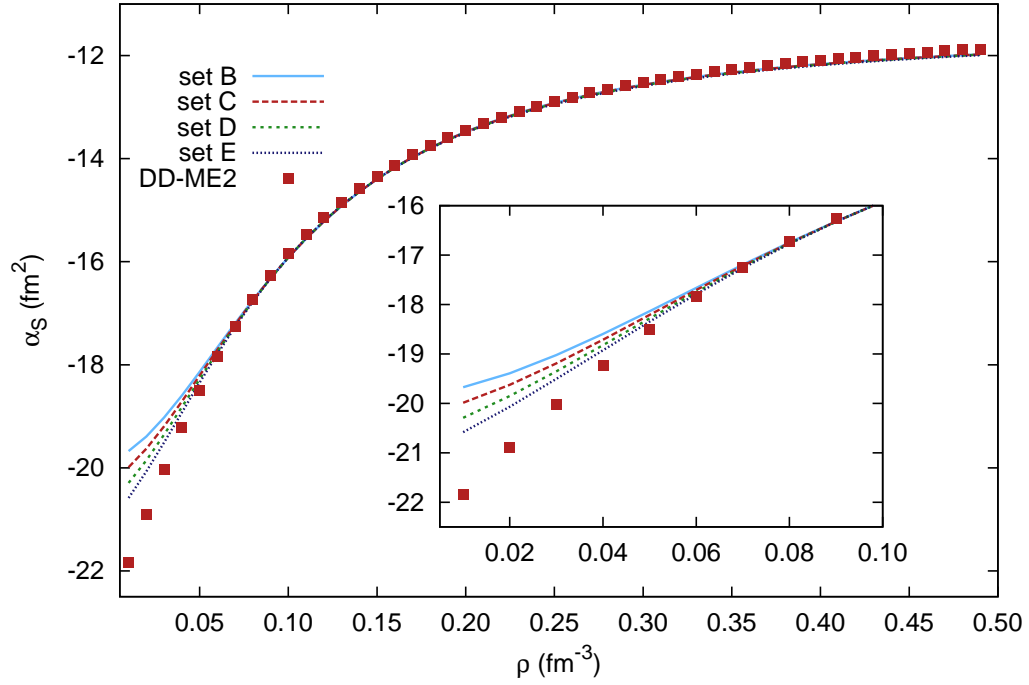


FIG. 2: The density dependence of the isoscalar-scalar coupling α_S for the meson-exchange interaction DD-ME2, and the four point-coupling parameter sets (cf. Table III). The differences in the low-density region are emphasized in the insert.

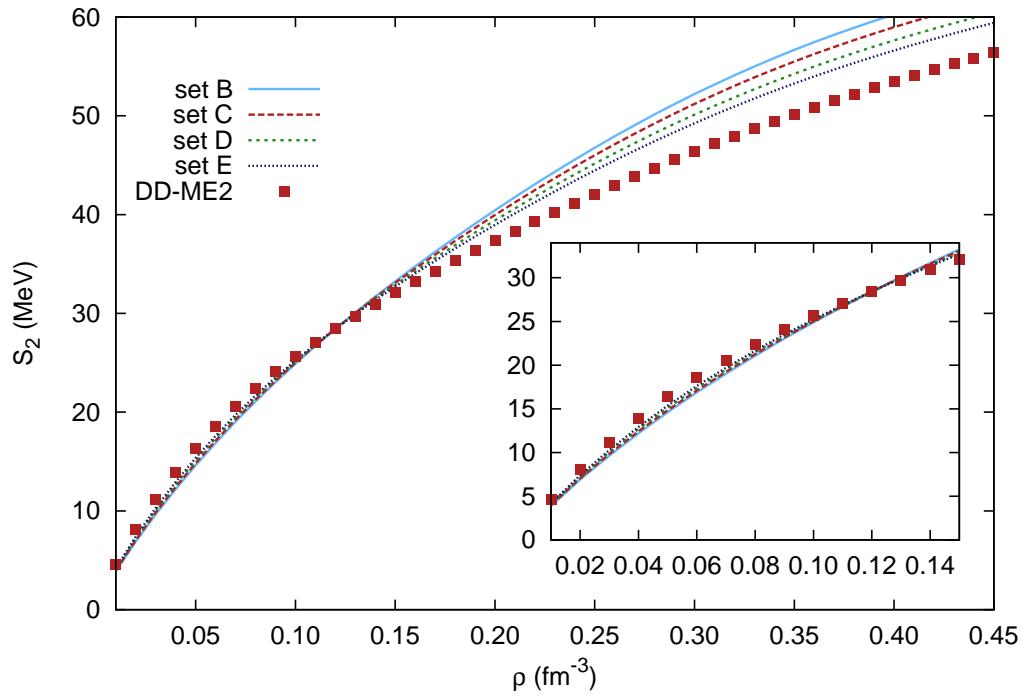


FIG. 3: The symmetry energy of nuclear matter as a function of nucleon density, for the meson-exchange interaction DD-ME2, and the four point-coupling parameter sets (cf. Table III). The density dependence below saturation density is shown in the insert.

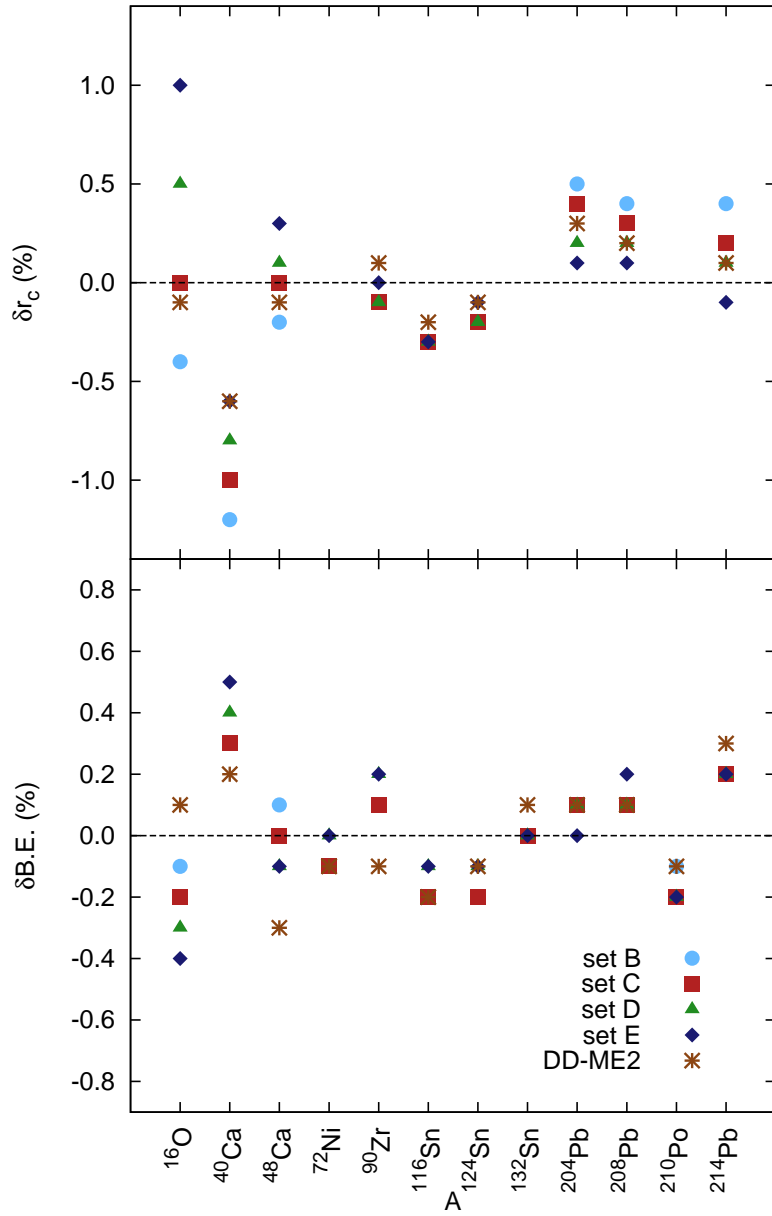


FIG. 4: The deviations (in percentages) between the experimental and theoretical charge radii (upper panel), and binding energies (lower panel) of 12 spherical nuclei, calculated with the meson-exchange interaction DD-ME2, and the four point-coupling parameter sets (cf. Table III).

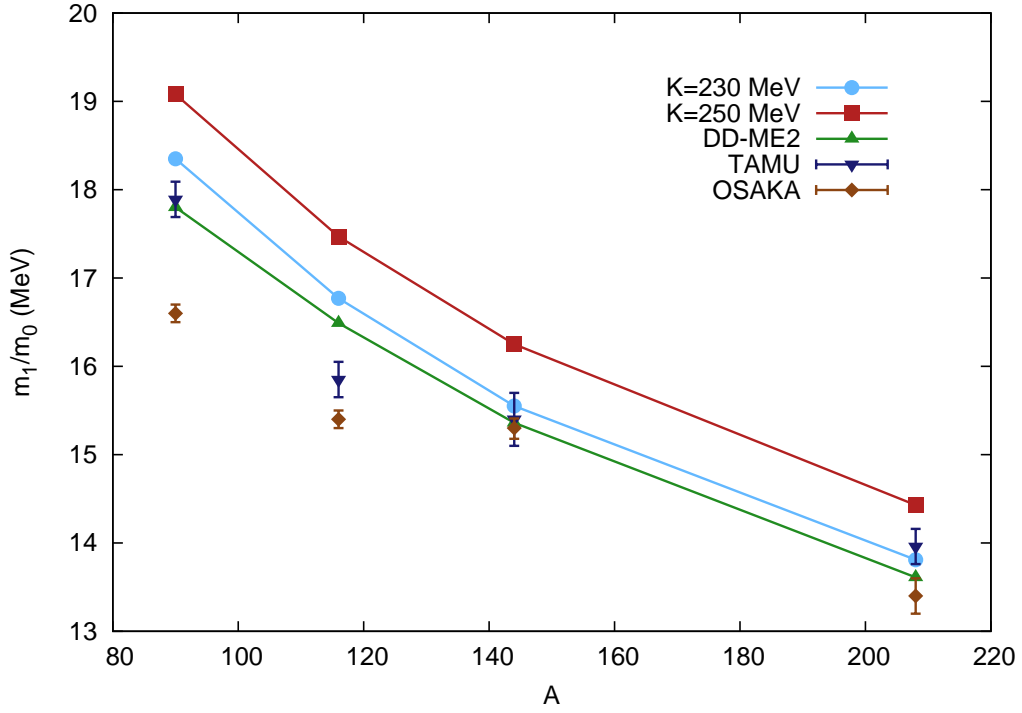


FIG. 5: The RQRPA results for the ISGMR centroid energies (m_1/m_0) of ^{90}Zr , ^{116}Sn , ^{144}Sm , and ^{208}Pb , calculated with the relativistic DD-ME2 meson-exchange interaction ($K_{nm} = 251$ MeV), and with two point-coupling effective interactions: set F ($K_{nm} = 250$ MeV) and set G ($K_{nm} = 230$ MeV). The theoretical results are compared with data from the TAMU [22, 23, 24] and Osaka [25, 26] compilations.

TABLE I: The parameters of the point-coupling effective interaction (set A) that, on the nuclear matter level, is completely equivalent to the meson-exchange interaction DD-ME2.

Set A	
α_S (fm ²)	-14.3275
b_S	0.9119
c_S	2.1127
d_S	0.3882
δ_S (fm ⁴)	
α_V (fm ²)	10.7963
b_V	0.7648
c_V	1.8199
d_V	0.4115
α_{TV} (fm ²)	0.9076
a_{TV}	1.1294

TABLE II: The surface thickness and surface energy of semi-infinite nuclear matter, calculated with the point-coupling effective interaction (parameter set A) for various values of the strength δ_s of the derivative term, in comparison with the values predicted by the DD-ME2 meson-exchange interaction.

δ_S (fm ⁴)	t (fm)	a_s (MeV)
-0.76	2.125	15.32
-0.78	2.157	15.57
-0.80	2.189	15.82
-0.82	2.221	16.06
-0.84	2.254	16.29
-0.86	2.286	16.52
DD-ME2	2.108	17.72

TABLE III: The parameters of the isoscalar-scalar and isovector-vector channels of point-coupling effective interactions, adjusted to the nuclear matter equation of state, symmetry energy, and ground-state properties of finite nuclei. See text for the description.

	set A	set B	set C	set D	set E	set F	set G
b_S	0.9119	1.0277	1.0097	1.0010	1.0011	1.0028	1.1030
c_S	2.1127	1.7692	1.7839	1.8169	1.8674	1.8056	1.9386
d_S	0.3882	0.0674	0.1074	0.1452	0.1796	0.1344	0.0907
δ_S (fm ⁴)		-0.80	-0.82	-0.84	-0.86	-0.8342	-0.8445
α_{TV} (fm ²)	0.9076	0.9883	0.9764	0.9618	0.9500	0.9658	0.9765
a_{TV}	1.1294	0.7059	0.7663	0.8368	0.8992	0.8166	0.8439

TABLE IV: The surface thickness and surface energy of semi-infinite nuclear matter, calculated with the point-coupling effective interactions: parameter sets B, C, D, and E (cf. Table III).

	t (fm)	a_s (MeV)
set B	2.015	17.925
set C	2.069	17.856
set D	2.126	17.780
set E	2.184	17.717

TABLE V: The total binding energies ($B.E.$), charge radii r_c , and the differences between the radii of neutron and proton density distributions $r_{np} = (r_n - r_p)$, used to adjust the parameters of the point-coupling effective interactions. The values calculated with the parameter set G (cf. Table III) are compared with data (values in parentheses). In the last three columns the corresponding deviations dE , dr_c , and dr_{np} (all in percentages) are included.

Nucleus	$B.E.$ (Mev)	r_c (fm)	$r_n - r_p$ (fm)	dE	dr_c	dr_{np}
^{16}O	127.21 (127.62)	2.74 (2.73)	-0.03	-0.3	0.5	
^{40}Ca	343.77 (342.05)	3.46 (3.48)	-0.05	0.5	-0.8	
^{48}Ca	415.76 (415.99)	3.49 (3.48)	0.19	-0.1	0.1	
^{72}Ni	612.74 (613.17)	3.92	0.31	-0.1		
^{90}Zr	785.70 (783.89)	4.27 (4.27)	0.08	0.2	-0.1	
^{116}Sn	987.90 (988.68)	4.61 (4.63)	0.12 (0.12)	-0.1	-0.3	0.0
^{124}Sn	1048.88 (1049.96)	4.67 (4.67)	0.21 (0.19)	-0.1	-0.2	12.3
^{132}Sn	1102.66 (1102.86)	4.72	0.25	0.0		
^{204}Pb	1609.11 (1607.52)	5.50 (5.49)	0.17	0.1	0.3	
^{208}Pb	1639.39 (1636.45)	5.52 (5.51)	0.19 (0.20)	0.2	0.2	-6.5
^{214}Pb	1659.97 (1663.29)	5.57 (5.56)	0.24	-0.2	0.1	
^{210}Po	1649.71 (1645.23)	5.55	0.17	0.3		